ARCHIVES
of
FOUNDRY ENGINEERING

ISSN (2299-2944)

10.24425/afe.2024.151294

Published quarterly as the organ of the Foundry Commission of the Polish Academy of Sciences

Research into the Structure and Adhesion of WCCoCr Coatings Plasma-Sprayed onto Castings of AlSi Alloy Plates

M. Radoń *, Z. Opiekun, B. Kupiec
Rzeszow University of Technology,
Al. Powstańców Warszawy 12, 35-959 Rzeszów, Poland
* Corresponding author. E-mail address: m.radon@prz.edu.pl

Received 20.03.2024; accepted in revised form 22.07.2024; available online 11.09.2024

Abstract

The article presents structural investigations and mechanical properties of hard coatings deposited by spraying WCCoCr powder in an argon-hydrogen plasma jet onto the surfaces of AlSi10Mg alloy casting plates.
Two variants (A and B) of processing parameters of the powder spraying process onto the surface of silumin plates were applied, resulting in different coating thickness. The coating applied according to variant A was done with 12 passes, and its thickness was approximately 150 µm. The coating applied according to variant B was done with 20 passes, and its thickness was about 320 µm. The microstructures of these coatings are similar, consisting of wavy, alternately deposited phases of solid solutions with varying concentrations of elements, and fine spherical phases, irregularly dispersed carbides. A qualitative analysis of the distribution of microstructure components was performed based on surface mapping. Precipitates differing in their degree of grayness and shape were identified based on microanalysis of their chemical composition. The porosity assessment of coatings performed in five randomly selected areas amounts to an average of 9%.
The applied coatings exhibit good adhesion to the substrate, as evidenced by the absence of delamination during scratching tests using a diamond Rockwell indenter loaded with a force of 10 N. The coating hardness averaged 1180HV0.2.
The test results indicate the high quality of the WCCoCr coatings, regardless of their thickness.

Keywords: WCCoCr coatings, Aluminium cast alloy, Atmospheric plasma spraying

1. Introduction

Plasma spraying of coatings applied to components made of various structural materials is often carried out using the APS (Air Plasma Spraying) method. The APS process is stable and highly efficient. In this process, the material being sprayed is typically a powder with different granulometric fractions (from 2 to about 100 µm and larger) [1,2], and the plasma-forming gases are argon, hydrogen, and helium. The APS method has found applications in many industries (automotive, aerospace, defence, electronics, nuclear energy, etc.).

Many processing factors [3] affect the functional properties of coatings obtained by plasma spraying of powders, of which the most important are preparation of the surface of the component before the spraying process, intensity of plasma flow and temperature, amount of powder fed (g/min), shape and size of powder particles [4], distance of the torch nozzle from the sprayed surface, and torch movement speed [5].

In the automotive industry, pistons for internal combustion engines are cast from eutectic silumin. Due to their very harsh

operating conditions such as exposure to high temperatures [6] and erosive-corrosive effects of exhaust gases, various coatings are applied to pistons to improve their functional properties [7-10]. For example, coatings of 8%Y_2O_3-ZrO_2 with thickness ranging from 50 to 250 µm serve as thermal barrier coatings [11-12]. These coatings reduce the thermal conductivity coefficient, contribute to fuel consumption reduction and exhaust emission, and also enhance the resistance of these structural components to thermal fatigue.

Coatings based on tungsten carbide WC thermally sprayed by HVOF or HVAF methods onto the inner surfaces of engine cylinders aim to extend the lifespan of these components by reducing fretting wear [13].

The use of hard coatings based on tungsten carbide, according to the authors of [14], also improves the resistance to erosive wear. The test results proved that the coatings have significantly better erosion resistance than the magnesium alloy substrate.

In corrosion tests carried out by the authors of work [15,16], it was observed that the corrosion resistance of coatings increases with the increase in the amount of WCCo in the coating layer.

The wide use of WC-based coatings means that interest in such surface modification methods is constantly developing, hence the aim of this work was to determine the possibility of applying WCCoCr powder coatings by plasma spraying (APS).

The research included: substrate preparation, application of two coatings using different processing parameters of the APS process, analysis of microstructure and chemical composition of the substrate and coatings. The quality assessment of the coating-substrate bond (adhesion) was carried out by diamond scratching from the substrate towards the coating.

2. Research material and methodology

The research material consisted of castings of plates made of AlSi10Mg alloy, covered by the PN-EN 1706-2022 standard (Aluminium and aluminium alloys – Castings – Chemical composition and mechanical properties). The chemical composition of the plates on which the coatings were applied is presented in Table 1. The analysis of the chemical composition of the substrate material was performed using a Q4 Tasman Bruker optical spectrometer.

Table 1.
Results of chemical composition analysis of AlSi10Mg alloy

Si, %	Mg, %	Mn, %	Fe, %	Ti, %	Al, %
10.6	0.3	0.4	0.52	0.15	balance

The surfaces of the plate castings were subjected to abrasive jet machining. Machining was carried out using the KCW-1200-1150+FCPd device. This machining involved the action of electrocorundum particles with grain sizes of 125-180 µm in an air stream, at a pressure of about 3.5 bar. The distance of the abrasive nozzle from the surface of the plates was about 100 mm, and the duration of the abrasive action was 30 s. These parameters for preparing the surfaces of the plates ensured their uniform roughness, determined by the parameter S_t (surface roughness) at the level of 14-23 µm. Immediately after abrasive jet machining of the AlSi10Mg alloy plates, the plasma spraying process in coatings was carried out using a robotised SULZER METCO station equipped with an ABB robot, F4-MB-HBS torch, and powder feeder.

The material for coating was WCCoCr 86104 powder from Thermico, which contained approximately 40% spherical particles with a diameter of 2-20µm and approximately 60% particles with polyhedral shapes. An example view of the powder particles is shown at Figure 1. According to the manufacturer's data, the powder contained 86% WC, 10% Co, and 4% Cr.

Coatings on the castings of AlSi10Mg alloy plates were sprayed in two variants designated as variant A and variant B. Table 2 presents the developed processing parameters of the spraying process.

Metallographic studies were conducted on metallographic specimens obtained by mechanical polishing of cross-sectional cuts of castings of plates with applied coatings. The analysis was carried out using a TESCAN Vega 3 scanning microscope with an INCA X-ACT OXFORD attachment for microanalysis of chemical composition. To reveal the microstructure of the substrate, specimens were etched with a 4% aqueous solution of hydrofluoric acid.

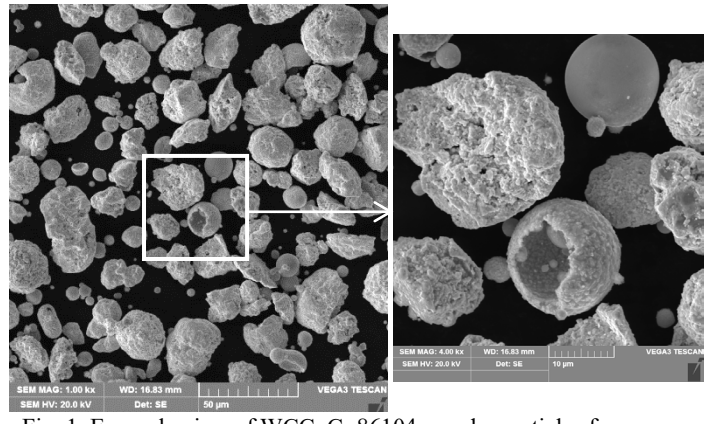

Fig. 1. Example view of WCCoCr 86104 powder particles from Thermico, containing 86% WC, 10% Co, and 4% Cr

Table 2.
Technological parameters of plasma spraying coatings on AlSi10Mg alloy plates

Parameter	Variant A	Variant B
Carrier gas, l/min:	4	4
Powder feeder disk speed, rpm:	0.9	0.9
Current intensity, A:	650	650
Argon flow rate, l/min:	60	60
H_2 Hydrogen flow rate, l/min:	7	7
Air jet pressure, bar:	2	2
Spraying distance, mm:	110	110
Linear velocity of the torch, mm/min:	190	190
Coating thickness, µm:	120-145	298-325
Number of torch passes:	12	20

The quality assessment of the substrate-coating connection (adhesion testing) was conducted using the REVETEST RST device (CSM Instruments), where a diamond indenter, Rockwell cone, under a load of 10N, scratched the surface according to the

scheme shown at Figure 2. The indenter was moved at a speed of 0.5 mm/min.

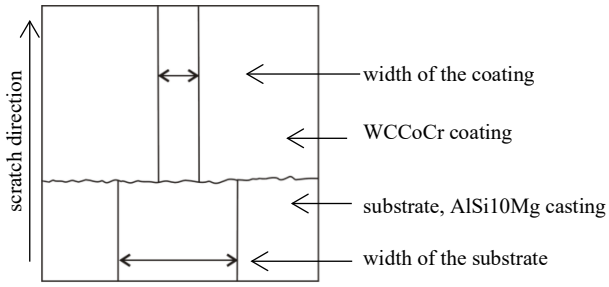

Fig. 2. Adhesion testing scheme in substrate-coating connection

Coating hardness was measured using a Vickers hardness tester ZHV10, applying a 10N load.

3. Test results

An exemplary microstructure of the AlSi10Mg alloy is presented at Figure 3. This is a typical microstructure of approximately eutectic silumin, consisting of dendrites of α(Al) phase and eutectic α(Al)+β(Si) distributed along the boundaries of these dendrites.

Figures 4 and 5 show exemplary microstructures of cross-sectional cuts of castings of AlSi10Mg alloy plates with coatings applied according to variant A and variant B.

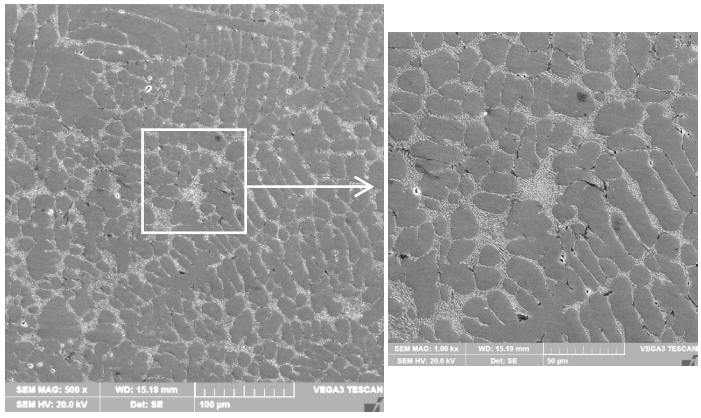

Fig. 3. Exemplary microstructure of AlSi10Mg alloy

To analyze the surface distribution of elements in the coating shown at Figure 6, an area containing all visible precipitates occurring in the cross-section of both coatings was selected.
In order to identify individual coating precipitates, an additional microanalysis of the chemical composition was performed using a scanning microscope. Typical areas present in both coating variants were selected to perform this analysis. Figure 7 shows a selected view of the coating and the results of microanalysis of its chemical composition.

Observations of scratches made by the diamond Rockwell indenter, moving on the surface of the metallographic specimen from the substrate material towards the WCCoCr coating surface, made according to variant A and variant B, are presented at Figures 8 and 9.

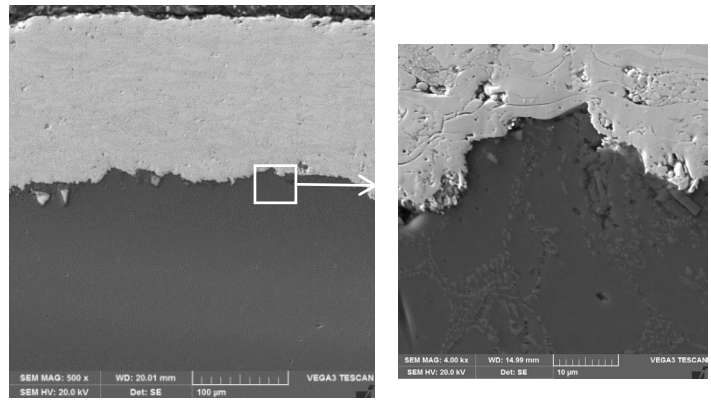

Fig. 4. View of the substrate-coating connection made according to variant A

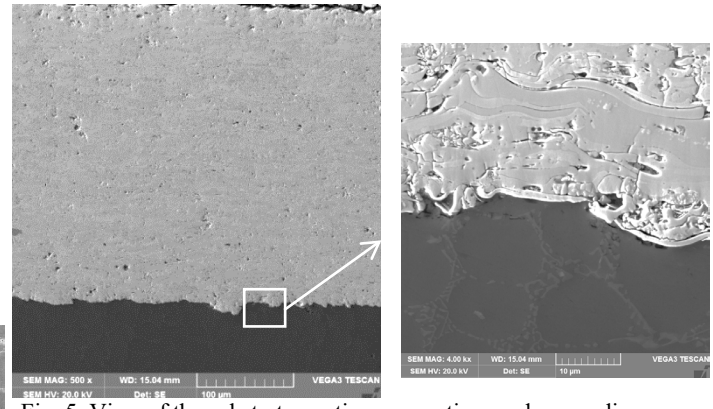

Fig. 5. View of the substrate-coating connection made according to variant B

The qualitative analysis of the distribution of elements in the WCCoCr coating revealed that the highest concentration of chromium occurs as a dark gray precipitate (Fig. 6c). In slightly lighter precipitates, a high concentration of cobalt can be seen (Fig. 6d), while tungsten is distributed evenly over the entire surface of the coating (Fig. 6b).

The qualitative analysis of the surface distribution of elements is confirmed by the results of microanalysis of the chemical composition of individual precipitates. The specified carbon content as a percentage (weight%) of the chemical composition is indicative due to the limitations of the research method used. The microstructures of the analyzed coatings are similar, consisting of wavy, alternatingly deposited phases of solid solutions with different concentrations of elements, and small spherical phases, irregularly distributed carbides embedded in a cobalt matrix.

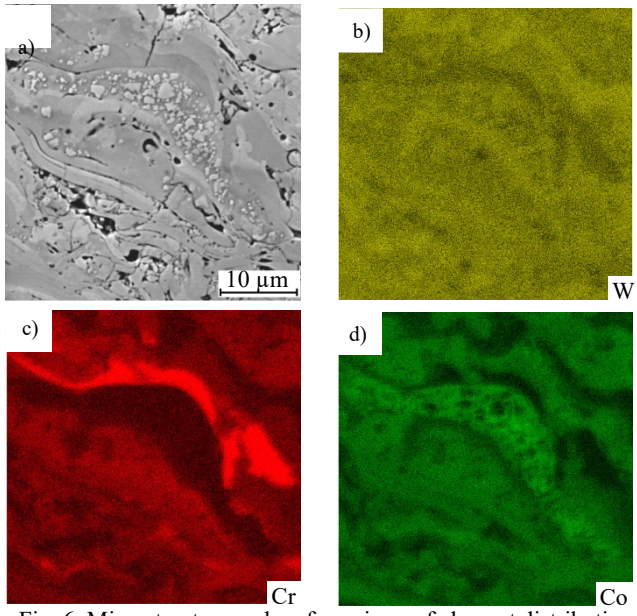

Fig. 6. Microstructure and surface views of element distribution: tungsten (b), chromium (c), and cobalt (d)

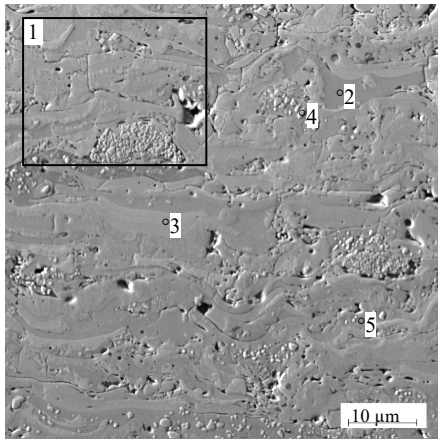

Point	C, %	Cr, %	Co, %	W, %
1	5,33	1,71	3,73	bal.
2	5,26	26,62	3,41	bal.
3	3,56	8,31	12,19	bal.
4	5,21	0,80	1,06	bal.
5	1,88	0,04	84,35	bal.

Fig. 7. Results of X-ray microanalysis of the chemical composition of the WCCo coating

In order to supplement the information about the quality of the coatings, an additional porosity assessment was performed. The analysis was carried out on metallographic sections using a scanning microscope with a magnification of 2000x. Measurements were made for five randomly selected areas, each with an area of 8262 µm2.

Porosity was determined as a percentage by the ratio of the pore area to the area of the examined area.

The results of the porosity assessment of both variants of the coatings were similar and amounted to an average of 9%.

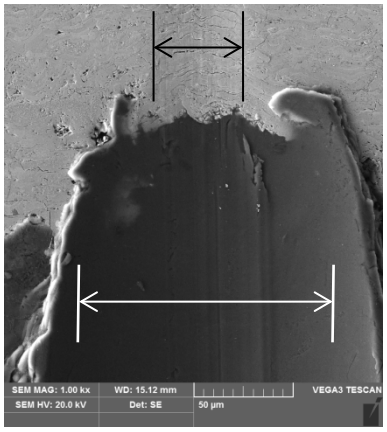

Fig. 8. View of scratching in the substrate-coating transition zone, made according to variant A

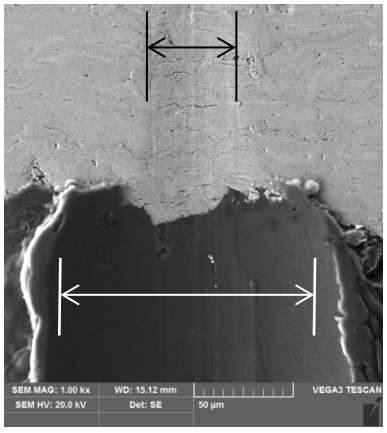

Fig. 9. View of scratching in the substrate-coating transition zone, made according to variant B

Observations in the transition zone: substrate and coating in both variants of their execution do not reveal delamination. The coating material is much less susceptible to scratching and the same widths of scratches are observed both on the AlSi alloy substrate and in the coating.

The width of scratches in the substrate was about 155 µm, while in the coatings, it was about 50 µm.

In the case of an AlSi alloy substrate, characteristic flashes are observed caused by material being drawn in by the indenter.

4. Summary

The result of plasma-sprayed surfaces of AlSi10Mg alloy plate castings with WCCoCr powder are coatings with thickness of approximately 137 and 312 µm. The average hardness of these coatings is 1180 HV0.2, which is approximately ten times greater

than the hardness of the substrate, the AlSi10Mg alloy casting. The coatings exhibit good adhesion, as evidenced by their lack of detachment from the substrate surface during scratching tests. The coatings have a wavy strip structure. These strips consist of tungsten solid solutions with varying concentrations of chromium and cobalt. In the interstrip spaces, the presence of very fine, spherical, unevenly distributed tungsten-rich carbides is observed. Small amounts of pores are also present at the interface of the wavy layers.

References

[1] Sokołowski, P., Łatka, L., Kozerski, S. & Ambroziak, A. (2015). Plasma spraying from slurries as an alternative to conventional powder plasma spraying. *Spajanie materiałów konstrukcyjnych.* 3(29), 28-31. (in Polish).

[2] Dudek, S., Gancarczyk, T. & Sosnowy, P. (2012). Application of thermal spraying on the example of a turbine engine. *Welding Technology Review.* 84(9), 9-13. DOI: https://doi.org/10.26628/wtr.v84i9.351. (in Polish).

[3] Bakan, E. & Vaßen, R. (2017). Ceramic top coats of plasma-sprayed thermal barrier coatings: materials, processes, and properties. *Journal of Thermal Spray Technology.* 26, 992-1010. DOI: https://doi.org/10.1007/s11666-017-0597-7.

[4] Heimann, R. (2008). *Plasma Spray coating: principles and applications* (2nd ed.). German-Weinhem: Willey-VCH.

[5] Mróz, M. & Rąb, P. (2023). Evaluation of the possibility of applying thermal barrier coatings to AlSi7Mg alloy castings. *Archives of Foundry Engineering*. 23(3), 104-109. DOI: 10.24425/afe.2023.146668.

[6] Pierce, D., Haynes, A., Hughes, J., Graves, R., Maziasz, P., Muraligharan, G., Shyam, A., Wang, B., England, R. & Daniel, C. (2018) High temperature materials for heavy duty diesel engines: historical and future trends. *Progress in Materials Science.* 103, 109-179. DOI: 10.1016/j.pmatsci.2018.10.004.

[7] Tan, L.G., Li, G.L., Tao, C. & Feng, P.F. (2022). Study on fatigue life prediction of thermal barrier coatings for high-power engine pistons. *Engineering Failure Analysis*. 138, 106335. DOI: https://doi.org/10.1016/j.engfailanal.2022.106335.

[8] Padture, N.P., Gell, M. & Jordan, E.H. (2002). Thermal barrier coatings for gas-turbine engine applications. *Science.* 296(5566), 280-284. DOI: 10.1126/science.1068609.

[9] de Goes, W.U., Markocsan, N., Gupta, M., Vassen, R., Matsushita, T. & Illkova, K. (2020). Thermal barrier coatings with novel architectures for diesel engine applications. *Surface and Coatings Technology*. 396, 125950. DOI: 10.1016/j.surfcoat.2020.125950.

[10] Uczak de Goes, W., Somhorst, J., Markocsan, N., Gupta, M. & Illkova, K. (2019). Suspension plasma-sprayed thermal barrier coatings for light-duty diesel engines. *Journal of Thermal Spray Technology.* 28, 1674-1687. https://doi.org/10.1007/s11666-019-00923-8.

[11] Opiekun, Z. (2014). Mechanical properties of the thermal barrier coatings made of cobalt alloy MAR-M509. In M. Aliofkhazraei (Eds.). *Superalloys* (331-335). Iran, Techeran. IntechOpen. DOI: 10.5772/61100.

[12] Reghu, V.R., Shankar, V. & Ramaswamy, P. (2018). Challenges in plasma spraying of 8% Y_2O_3-ZrO_2 thermal barrier coatings on al alloy automotive piston and influence of vibration and thermal fatigue on coating characteristics. *Materials Today: Proceedings*. 5(11), 23927-23936. DOI: 10.1016/j.matpr.2018.10.185.

[13] Reghu, V.R., Lobo, K., Basha, A., Tilleti, P., Shankar, V. & Ramaswamy, P. (2019). Protection offered by thermal barrier coatings to Al-Si alloys at high temperatures–A microstructural investigation. *Materials Today: Proceedings*. 19(2), 676-681. DOI: 10.1016/j.matpr.2019.07.752.

[14] Pulsford, J., Venturi, F., Pala, Z., Kamnis, S. & Hussain, T. (2019). Application of HVOF WC-Co-Cr coatings on the internal surface of small cylinders: Effect of internal diameter on the wear resistance. *Wear.* 432-433, 202965. DOI: 10.1016/j.wear.2019.202965.

[15] Jonda, E., Łatka L., Lont A., Gołombek K., Szala M. (2024). The effect of HVOF spray distance on solid particle erosion resistance of WC-based cermets bonded by Co, Co-Cr and Ni deposited on mg-alloy substrate. *Advances in Science and Technology Research Journal.* 18(2), 115-128. DOI: https://doi.org/10.12913/22998624/184025.

[16] Akkaş M. (2020). The mechanical and corrosion properties of WCCo–Al coatings formed on AA2024 using the HVOF method. *Material Research Express*. 7(7), 076515, 1-18. DOI 10.1088/2053-1591/ab9fba.